Heterogeneous Expression Patterns of the Minichromosome Maintenance Complex Members in Retinoblastoma Unveil Its Clinical Significance

Junjie Tang, Yaoming Liu, Zhihui Zhang, Yi Ren, Yujun Ma, Yinghao Wang, Jinmiao Li, Yang Gao, Cheng Li, Chao Cheng, Shicai Su, Shuxia Chen, Ping Zhang, and Rong Lu

State Key Laboratory of Ophthalmology, Zhongshan Ophthalmic Center, Sun Yat-Sen University, Guangdong Provincial Key Laboratory of Ophthalmology and Visual Science, Guangzhou, China

Correspondence: Rong Lu, State Key Laboratory of Ophthalmology, Zhongshan Ophthalmic Center, Sun Yat-Sen University, Guangdong Provincial Key Laboratory of Ophthalmology and Visual Science, 54 Xianlie S. Road, Guangzhou 510060, China; lurong@gzzoc.com.

JT and YL contributed equally to this work.

Received: October 10, 2023
Accepted: December 28, 2023
Published: January 17, 2024

Citation: Tang J, Liu Y, Zhang Z, et al. Heterogeneous expression patterns of the minichromosome maintenance complex members in retinoblastoma unveil its clinical significance. *Invest Ophthalmol Vis Sci.* 2024;65(1):31. https://doi.org/10.1167/iovs.65.1.31

Purpose. To explore the expression patterns and clinical significance of minichromosome maintenance (MCM) complex members in retinoblastoma (RB).

Methods. Single-cell RNA sequencing datasets from five normal retina, six intraocular, and five extraocular RB samples were integrated to characterize the expression patterns of MCM complex members at the single-cell level. Western blot and quantitative PCR were used to detect the expression of MCM complex members in RB cell lines. Immunohistochemistry was conducted to validate the expression of MCM complex members in RB patient samples and a RB mouse model.

Results. The expression of MCM2-7 is increased in RB tissue, with MCM2/3/7 showing particularly higher levels in extraocular RB. MCM3/7 are abundantly detected in cell types associated with oncogenesis. Both mRNA and protein levels of MCM3/4/6/7 are increased in RB cell lines. Immunohistochemistry further confirmed the elevated expression of MCM3 in extraocular RB, with MCM6 being the most abundantly expressed MCM in RB.

Conclusions. The distinct MCM expression patterns across various RB cell types suggest diverse functional roles, offering valuable insights for targeted therapeutic strategies. The upregulation of MCM3, MCM4, MCM6, and MCM7 in RB, with a specific emphasis on MCM6 as a notable marker, highlights their potential significance.

Keywords: retinoblastoma, minichromosome maintenance complex, single-cell transcriptomics

Retinoblastoma (RB) is a pediatric intraocular malignancy that originates from the inactivation of the *RB1* tumor suppressor gene during retinal development.[1] Its global annual incidence stands at approximately 1:15,000 to 1:20,000 cases.[2] Despite the considerable improvements in RB prognosis and treatment over recent decades, the challenge remains in effectively managing invasive RB, which current therapies have limited success in controlling.[3] In regions with limited resources, extraocular extension of RB remains relatively common owing to delayed diagnosis. This extension carries a notably higher mortality rate, especially when combined with metastatic disease or metastatic relapse.[4–6] Therefore, distinguishing the features of invasive RB is of paramount importance in clinical practice.

Genomic instability plays a role in tumor progression by generating genetic diversity within the tumor cell population.[7] This diversity can lead to the emergence of subpopulations of cancer cells with distinct characteristics, including resistance to treatments like chemotherapy.[8] The minichromosome maintenance (MCM) complex is composed of six members with similar structural characteristics, including MCM2, MCM3, MCM4, MCM5, MCM6, and MCM7, forming a hexagonal arrangement.[9] This complex plays a crucial role in coordinating DNA replication, functioning as a central regulator in this essential cellular process. Numerous studies have demonstrated that variations in MCM genes are associated with genomic instability and have implications for cancer prognosis.[10–13] Dysregulated expression and activation of MCM proteins are common findings in various malignancies, contributing to both genomic instability and uncontrolled progression of the cell cycle.[14] However, the specific prognostic value of individual MCM2 to MCM7 members in the development and progression of RB remains unclear.

Bioinformatics has opened up new avenues in cancer research, closely linked to genomics, proteomics, and pharmaceutical development. In recent years, single-cell RNA sequencing (scRNA-seq) technology has emerged as a powerful tool for studying the diverse cellular composition within the tumor microenvironment.[15] In this study, we used scRNA-seq data to examine the expression profiles of MCM complex members in RB at the single cell level.

Additionally, we identified key MCM proteins associated with tumor progression and invasion in RB.

Methods

scRNA-seq Data Processing and Integration

scRNA-seq data from four RB samples, consisting of two intraocular RB patients and two extraocular RB patients,[16] were combined with publicly available scRNA-seq datasets comprising five normal retina samples, four intraocular RB samples, and three extraocular RB samples.[17,18] Raw scRNA-seq reads underwent processing using Cell Ranger (version 6.0.2) software with default settings.[19] The Seurat R package (version 4.0.3) facilitated data integration.[20] After normalization, the top 2000 variable genes were selected using appropriate mean expression and dispersion thresholds. The "FindIntegrationAnchors" function identified common anchors across samples. These anchors were then used alongside the "IntegrateData" function to merge the datasets seamlessly into a single entity containing individual cells for subsequent analysis. Known gene markers from previous studies were used to determine specific cell types.[21–23] Differentially expressed genes (DEGs) were discerned among samples from distinct groups using the FindMarkers function within the Seurat package. Genes exhibiting a fold change greater than 1.5 and a Benjamini–Hochberg adjusted *P* value of less than 0.05 were deemed significant DEGs. The pseudotime trajectory was inferred using Monocle3 software.[24] Genes between distinct states were detected through the DifferentialGeneTest function (Q value < 0.001).

Clinical Samples

Written informed consent was secured from the patients' family members, and the study received approval from the Ethics Review Board of Zhongshan Ophthalmic Center (Guangzhou, China). All procedures adhered to the principles outlined in the Declaration of Helsinki. Human RB specimens were collected immediately after eye enucleation at Zhongshan Ophthalmic Center, and subsequent tissue dissection was performed to precisely isolate the tumor region for subsequent single-cell dissociation. Patients with or without involving retrobulbar optic nerve was first screened by imaging diagnosis before surgery and finally validated by pathological diagnosis after surgery.

Cell Lines

Two RB cell lines, WERI-Rb1 and Y79, along with a nontumor human retinal pigment epithelial cell line, ARPE-19 (American Type Culture Collection, Manassas, VA, USA), were used. Y79 and WERI-Rb1 cells were cultured in RPMI 1640 medium (Corning, USA) supplemented with 10% fetal bovine serum (Gibco, Thermo Fisher Scientific, Waltham, MA, USA) and 1% penicillin-streptomycin (Invitrogen, Waltham, MA, USA). ARPE-19 were cultured in Dulbecco's Modified Eagle Medium/Nutrient Mixture F-12 (Gibco, Thermo Fisher Scientific, Waltham, MA, USA) supplemented with 10% fetal bovine serum and 1% penicillin–streptomycin. All cells were incubated at 37°C with 5% CO_2.

Western Blotting

Proteins from tumor cells and tissues were extracted using RIPA lysis buffer (strong) (K1020, APE×Bio, Boston, MA, USA). Western blotting followed established protocols,[25] employing specific antibodies for MCM3 (1:500, ZenBio [Durham, NC, USA], R22482), MCM4 (1:500, ZenBio, 160599), MCM6 (1:500, ZenBio, R22485), MCM7 (1:500, ZenBio, R24932), and GAPDH (1:10000, ProteinTech [Rosemont, IL, USA], 10494-1-AP). Membranes were probed with horseradish peroxidase–conjugated Affinipure Goat Anti-Rabbit IgG(H+L) (1:10000, ProteinTech, SA00001-2) for 1 hour, followed by three rounds of 10-minute washes in Tris-buffered saline 0.1% Tween-20. Visualization used enhanced chemiluminescence (ECL; Tanon, China) and the Tanon 5200 MultiImage System (Tanon, China).

RNA Extraction and Quantitative Real-time quantitative PCR (qPCR)

Total RNA was extracted using the EZBioscience EZ-press RNA Purification Kit (B0004D, EZBioscience, Roseville, MN, USA). RNA purity and concentration were evaluated using a Nanodrop 1000 spectrophotometer (Thermo Fisher Scientific). Subsequently, cDNA synthesis used 1000 ng total RNA and the EZBioscience 4 × Reverse Transcription Master Mix (A001GQ). The resultant reverse transcription product was mixed with other components in a 10 µl reaction for PCR amplification. PCR amplification involved initial heating to 95°C for 10 min, followed by 40 to 45 amplification cycles using specific primers. Each cycle encompassed denaturation at 95°C for 40 seconds, annealing at 53°C for 30 seconds, and extension at 72°C for 40 seconds (Roche, Basel, Switzerland). Data presented denote the relative mRNA abundance, normalized to the reference gene *GAPDH*. Primer sequences for each gene are available in Supplementary Table S1.

Orthotopic Xenograft Model

Animal experiments adhered to the ARVO Statement for the Use of Animals in Ophthalmic and Vision Research and were sanctioned by the Institutional Animal Care and Use Committee of Zhongshan Ophthalmic Center. For xenograft studies, BALB/c female nude mice (18–20 g body weight; 4–6 weeks old) were procured from Zhuhai BesTest Bio-Tech Co (Zhuhai, China) and maintained under specific pathogen-free conditions with climate control. Orthotopic RB xenografts were established as per a previously documented method.[25,26] Briefly, WERI-Rb1 cells (1×10^5 in 1 µL PBS) were injected onto the retina of right eye through a 33G Hamilton needle. Mice were euthanized after 28 days for enucleation.

Immunohistochemistry

Immunohistochemistry (IHC) was performed on 4-µm-thick paraffin sections of both human and mouse tissues using standardized protocols with optimized conditions. Tissue samples for the IHC analysis were collected from a total of 8 RB patients, comprising four intraocular RB patients and four extraocular RB patients who underwent treatment at Zhongshan Ophthalmic Center. The IHC staining of RB samples was assessed by two authors (J.T. and Y.L.). To quantify the expression of MCM3 (1:50, ZenBio, R22482), MCM4 (1:50, ZenBio, 160599), MCM6

Investigative Ophthalmology & Visual Science

(1:50, ZenBio, R22485), and MCM7 (1:50, ZenBio, R24932), Image J software (version 1.46; National Institutes of Health) was used for semiquantitative IHC analysis. The IHC analysis involved calculating the average optical density (AOD) value to measure the depth of MCMs (+) staining in RB cells.

Statistical Analysis

Data are expressed as means ± SD. Data analysis and visualization were conducted using the R software (R Foundation for Statistical Computing, Vienna, Austria, http://www.r-project.org) and GraphPad Prism Software v 8.0.2 (GraphPad, Inc., La Jolla, CA, USA). Statistical assessments involved unpaired two-tailed Student's *t* test and one-way ANOVA. Significance levels are indicated in the corresponding figures.

Results

Differential Expression of MCM Complex Members in RB

To identify clinically significant candidates associated with RB, a comprehensive analysis of MCM complex member expression, spanning MCM2-7, was conducted using scRNA-seq data. The scRNA-seq datasets comprised samples from five extraocular RB patients, six intraocular RB patients, and five normal retinas. After rigorous quality control procedures, including the removal of low-quality cells and doublets, a total of 128,454 qualified cells were retained. Among these, 55,492 and 61,882 cells were identified in extraocular and intraocular RB samples, respectively. A total of 1439 upregulated DEGs and 136 downregulated DEGs were identified in the RB samples. Among the upregulated DEGs, *TFF1*, *HIST1H4C*, and *TUBB* emerged as the

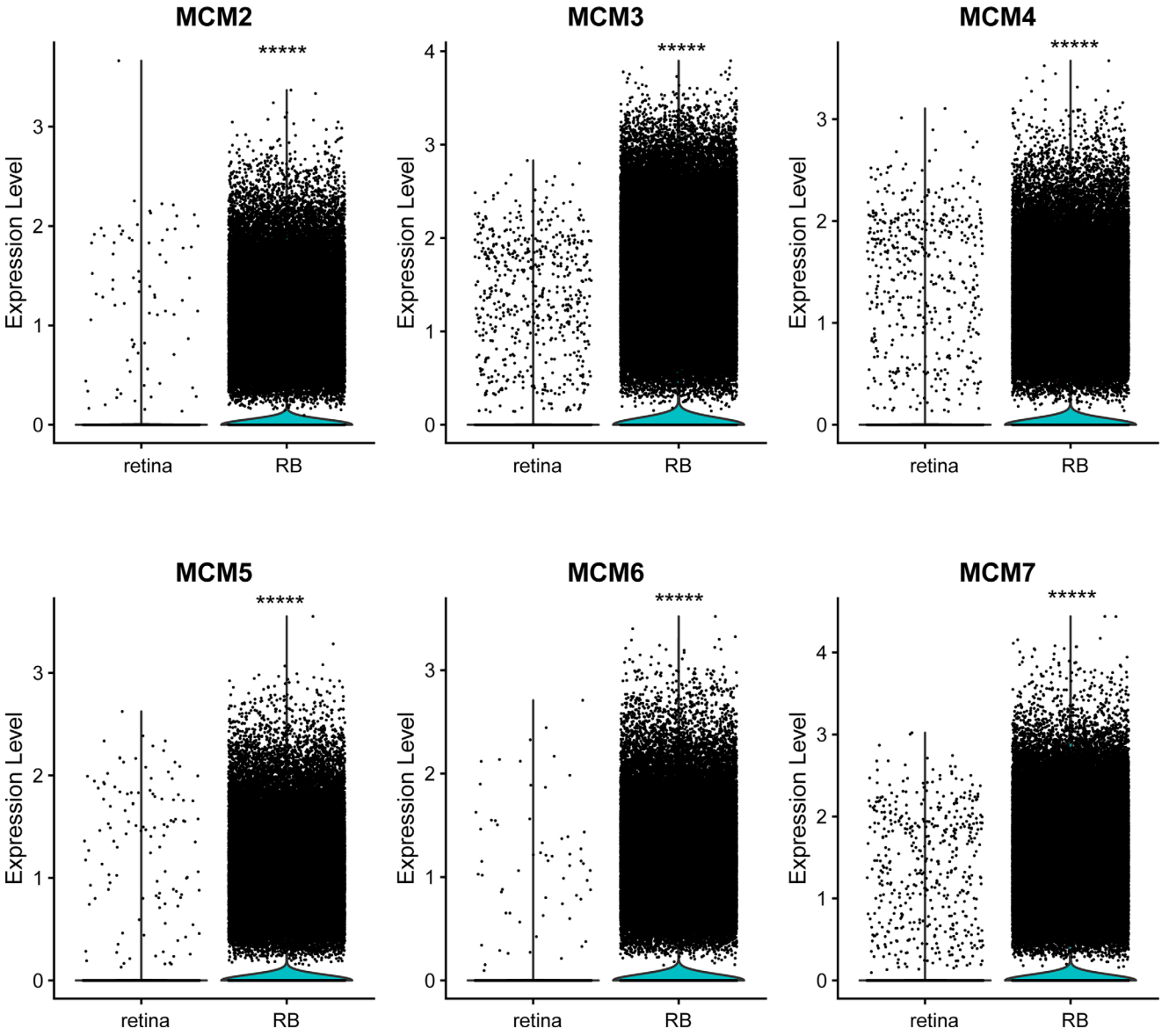

Figure 1. Differential expression of MCM complex members in RB. Comparative analysis of scRNA-seq data highlights the upregulation of all six MCM complex members (MCM2-7) in RB samples in comparison to normal retina. Significance assessed by unpaired, two-tailed Student's *t* test, with *P* values denoted as ****$P < 0.0001$.

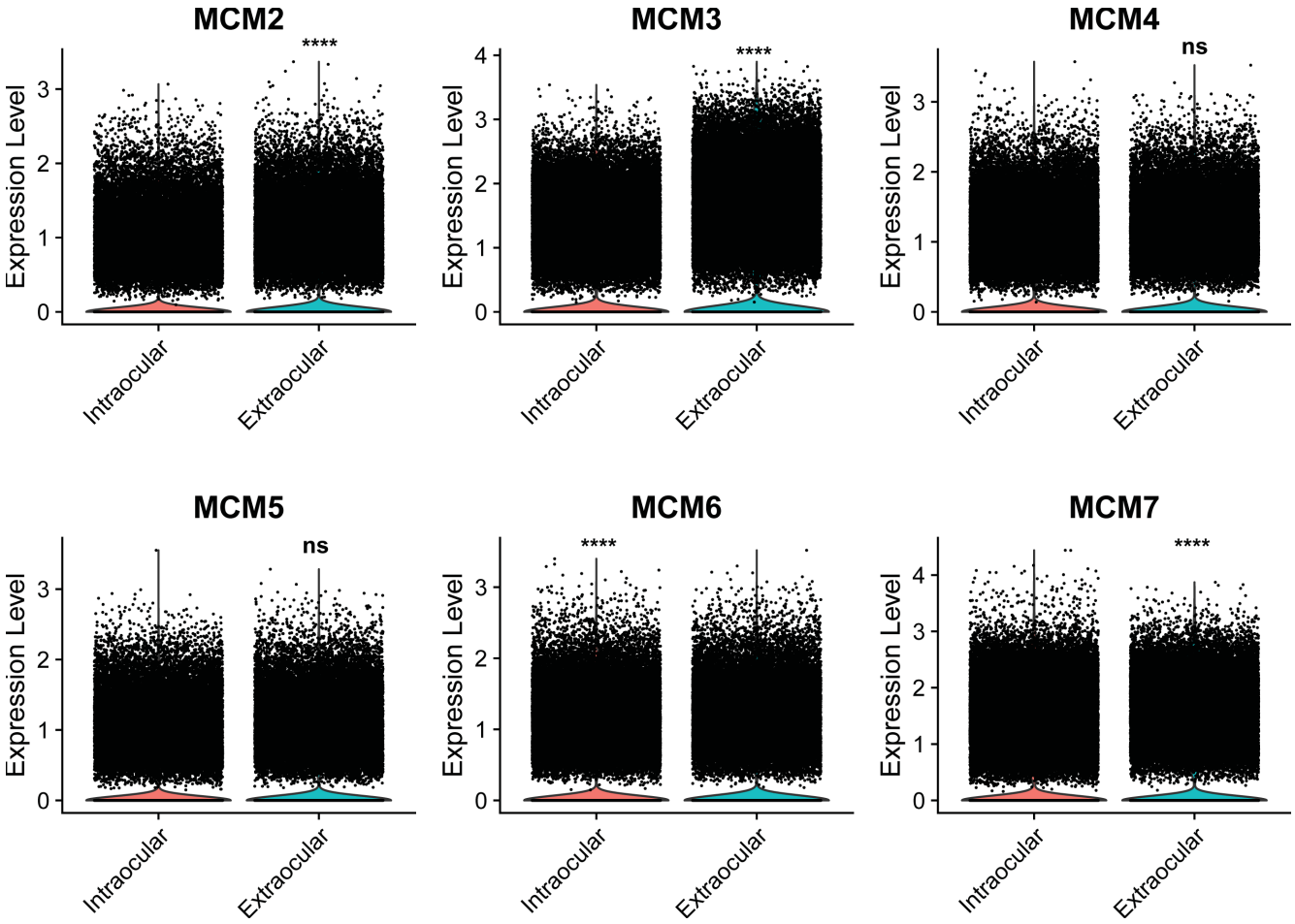

Figure 2. Comparative expression of MCM complex members in extraocular and intraocular RB. Notable differential expression of MCM complex members observed in extraocular RB in comparison with intraocular RB. Significance assessed by unpaired, two-tailed Student's *t* test, with *P* values denoted as ****$P < 0.0001$. ns, no significant difference.

most significant, whereas the most significant downregulated DEGs were *PDE6G*, *RHO*, and *SAG*, as depicted in Supplementary Figure S1A. Additionally, the results consistently reveal an upregulation pattern across all six MCM complex members in RB samples when compared with the normal retina (Supplementary Fig. S1B). For each member, the individual log2 fold changes (log2FC) and *P* values are as follows: MCM2 (log2FC = 0.83; $P = 0$), MCM3 (log2FC = 1.84; $P = 0$), MCM4 (log2FC = 1.13; $P = 0$), MCM5 (log2FC = 0.88; $P = 0$), MCM6 (log2FC = 1.14; $P = 0$), and MCM7 (log2FC = 1.88; $P = 0$) (Fig. 1). For a comprehensive overview, the list of DEGs between RB and the normal retina has been appended in the Supplementary File. Furthermore, when comparing extraocular RB with intraocular RB, it was observed that three MCM members were upregulated in extraocular RB: MCM2 (log2FC = 0.18; $P = 5.31E\text{-}121$), MCM3 (log2FC = 0.67; $P = 0$), and MCM7 (log2FC = 0.08; $P = 5.84E\text{-}84$) (Fig. 2).

Heterogeneous Expression of MCM Complex Members in Distinct RB Cell Types

Ten distinct cell types were identified using specific markers, including cone precursor-like cells, MKI67$^+$ photoreceptorness-decreased cells, rod precursor-like cells, retinoma-like cells, rods or rod-like cells, bipolar cells, Müller glia, microglia, and cones or cone-like cells. The expression patterns of MCM complex members exhibited heterogeneity across different cell clusters (Fig. 3A). Within the cell clusters of the normal retina, all members of the MCM complex manifested relatively low expression levels (Fig. 3B). Conversely, in the RB cell clusters, all MCM complex members showed elevated expression levels. Of particular note, MCM3 and MCM7 displayed significantly heightened expression levels in MKI67$_+$ photoreceptorness-decreased cells, rod precursor-like cells, cone precursor-like cells, and retinoma-like cells (Fig. 3C), suggesting their potential involvement in the regulation of these cell types. Branched expression analysis modeling analysis revealed a notably elevated expression level of MCM7 in both cone precursor-like cells and MKI67$^+$ photoreceptorness-decreased cells across pseudotime (Fig. 3D). However, this distinctive expression pattern was not observed in other cell types (Supplementary Fig. S2).

Overexpression of MCM Complex Members in RB Cell Lines

To gain deeper insights into the functional implications of MCM complex members in RB, we conducted an assessment

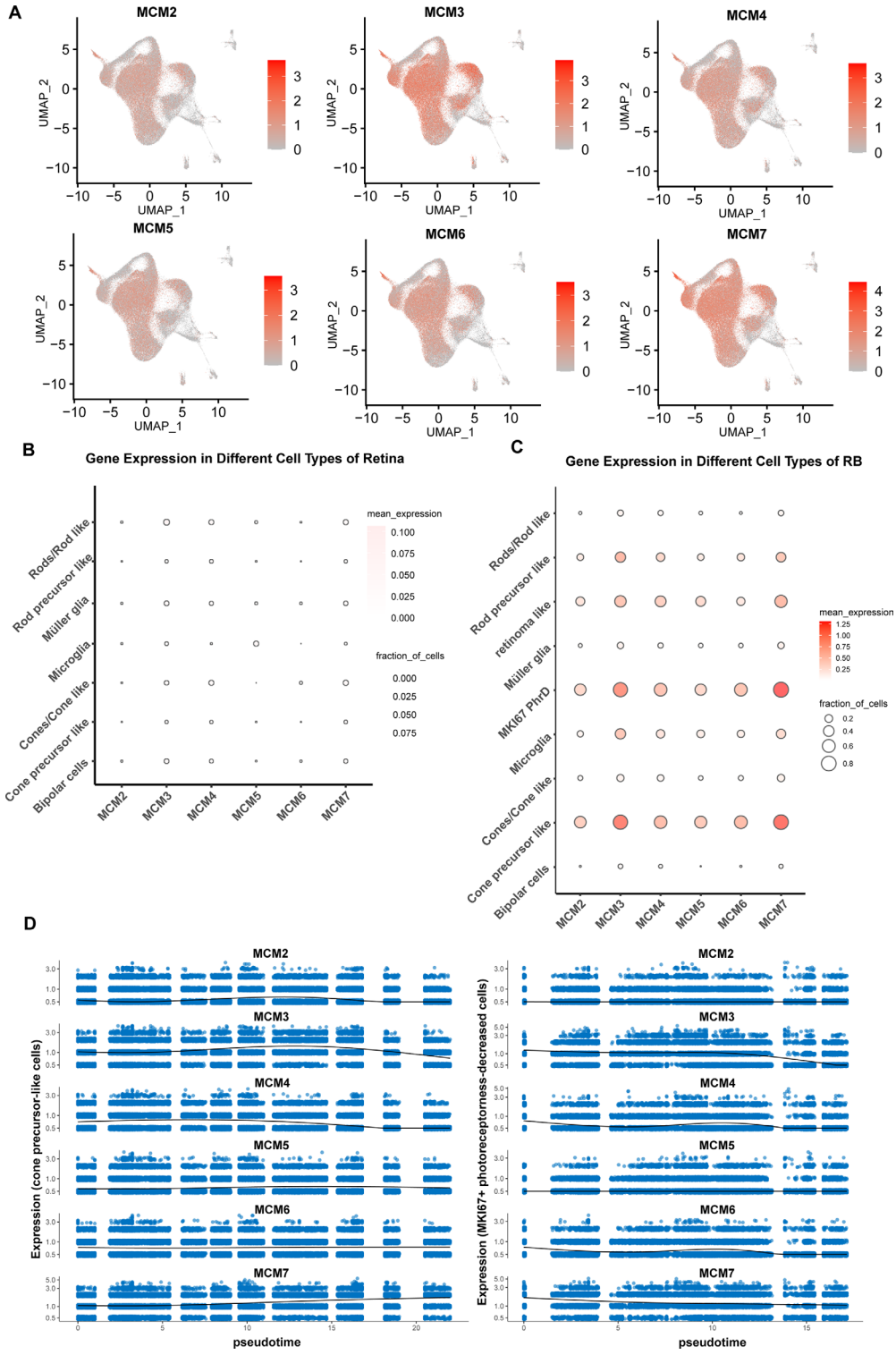

Figure 3. Heterogeneous expression of MCM complex members in distinct cell types. (**A**) Expression profiles of MCM complex members (MCM2-7) analyzed using integrated scRNA-seq datasets. (**B**) Expression patterns of MCM complex members in different cell types of normal retina. (**C**) Expression patterns of MCM complex members in different cell types of RB. (**D**) Pseudotime analysis reveals the trajectory of MCM complex members expression in malignant RB cell types.

of their expression in RB cell lines (WERI-Rb1 and Y79). Our qPCR assays revealed a notable upregulation of MCM3, MCM4, MCM6, and MCM7 in RB cell lines when compared with the control cell line ARPE-19 (Fig. 4A). These findings were further corroborated through Western blot analysis, which demonstrated significantly elevated levels of MCM3, MCM4, MCM6, and MCM7 proteins in RB cell lines (Fig. 4B). Collectively, these results provide compelling evidence for the pronounced overexpression of MCM3, MCM4, MCM6, and MCM7 in RB

Investigative Ophthalmology & Visual Science

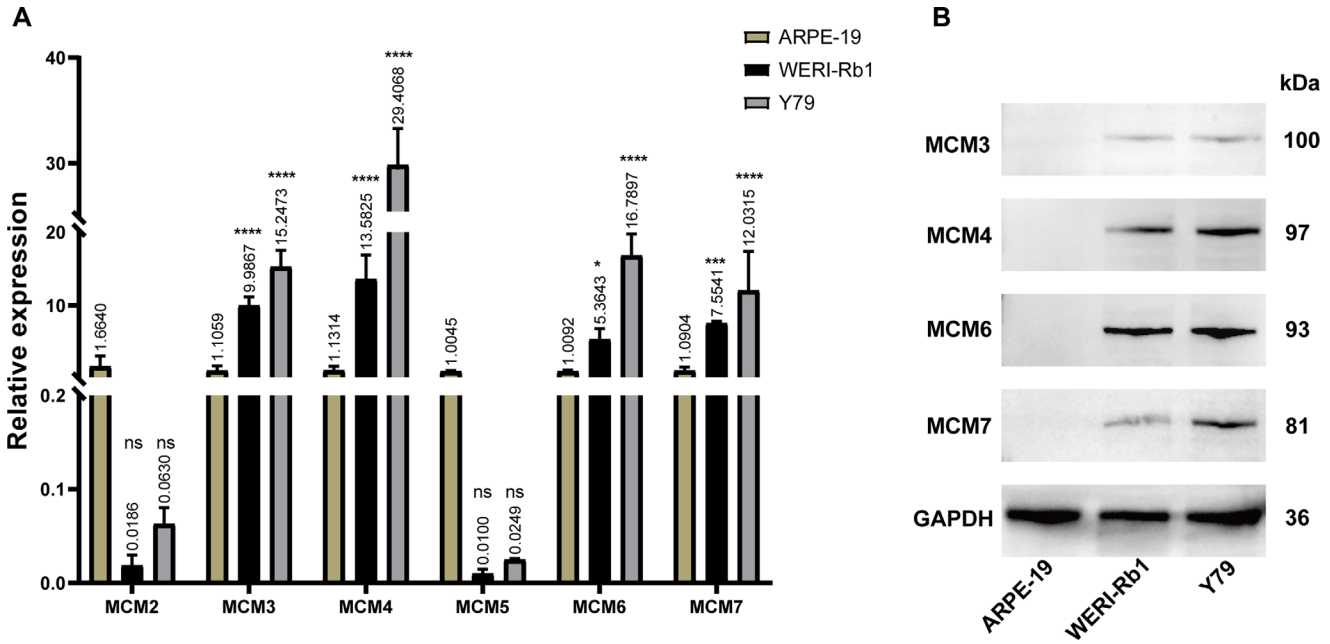

Figure 4. Overexpression of MCM complex members in RB cell lines. Elevated expression of MCM3, MCM4, MCM6, and MCM7 in RB cell lines (WERI-Rb1 and Y79) compared with the control cell line (ARPE-19), validated by (**A**) qPCR and (**B**) Western blot analysis.

cell lines, underscoring their potential functional relevance in RB.

Identification of Key MCM Proteins Associated With RB Development and Progression

Given the significant upregulation of MCM3, MCM4, MCM6, and MCM7 observed in both RB cell lines and scRNA-seq datasets (log2FC > 1), we proceeded with immunostaining for MCM3, MCM4, MCM6, and MCM7 on a set of four clinical samples diagnosed with intraocular RB, four samples diagnosed with extraocular RB, and four clinical samples from normal human retinas. The IHC analysis showed that the AOD of MCM3 was elevated in both intraocular and extraocular RB samples when compared with the normal retina, with extraocular RB demonstrating a particularly pronounced increase in MCM3 AOD compared with intraocular RB (Fig. 5A). Additionally, MCM4, MCM6, and MCM7 also exhibited heightened AOD in both intraocular and extraocular RB tissues relative to the normal retina, although no statistically significant differences were observed between extraocular RB and intraocular RB for these three MCM proteins (Figs. 5B–D). Among the four MCM proteins assessed, MCM6 displayed the most pronounced increase in AOD within RB samples (Fig. 5C). To further detect the role of MCM6 in RB development, WERI-Rb1 cells were injected intravitreally into BALB/c nude mice. Hematoxylin and eosin staining displayed that the tumor cells completely occupied both the vitreous cavity and the subretinal space, infiltrating the anterior chamber, cornea, and optic nerve (Fig. 6A). IHC staining demonstrated significant expression of MCM6 in the tumor tissue, although minimal expression was observed in noncancerous tissues such as the sclera, normal optic nerve, and retina (Fig. 6B). This finding suggests that MCM6 may serve as a potential marker for RB.

Discussion

Genomic instability is a significant factor in RB development and progression, highlighted by occurrences like *RB1* loss and *MYCN* amplification.[27] A decrease in the binding of the replicative helicase MCM complex 2 to MCM complex 7 at replication origins can induce replication stress and contribute to genome instability.[28] Although the role of the MCM complex in oncogenesis and prognosis has been validated partly in various cancers, a comprehensive analysis of the MCM complex in RB at the single-cell level is lacking. Importantly, emerging evidence emphasizes the significant role of tumor cell heterogeneity in RB and its impact on tumor progression.[29] In the present study, scRNA-seq data from five extraocular RB samples, six intraocular RB samples, and five normal retina samples were collected and processed. We conducted an analysis of scRNA-seq databases to investigate the expression of MCM2, MCM3, MCM4, MCM5, MCM6, and MCM7 in RB at both the tissue and single-cell levels. After this, we performed in vitro expression validation using RB cell lines through Western blotting and qPCR. Finally, we used IHC staining to further validate the results in both human and animal RB samples. Our findings revealed a widespread upregulation of MCMs in RB, with MCM6 consistently exhibiting a significant upregulation in all experimental validations, whereas MCM3 and MCM7 showed a potential association with tumor invasion.

Before the discovery of MCM protein functionality, standard cell proliferation markers included proliferating cell nuclear antigen (PCNA) and Ki-67. However, PCNA's involvement in DNA replication and repair interfered with its accuracy as a marker, reflecting cell proliferation activity.[30] Similarly, although many studies have associated Ki-67 with the proliferating cell growth phase, numerous functions of the Ki-67 antigen remain unknown. In contrast, the functions of the MCM protein family in the cell cycle, particu-

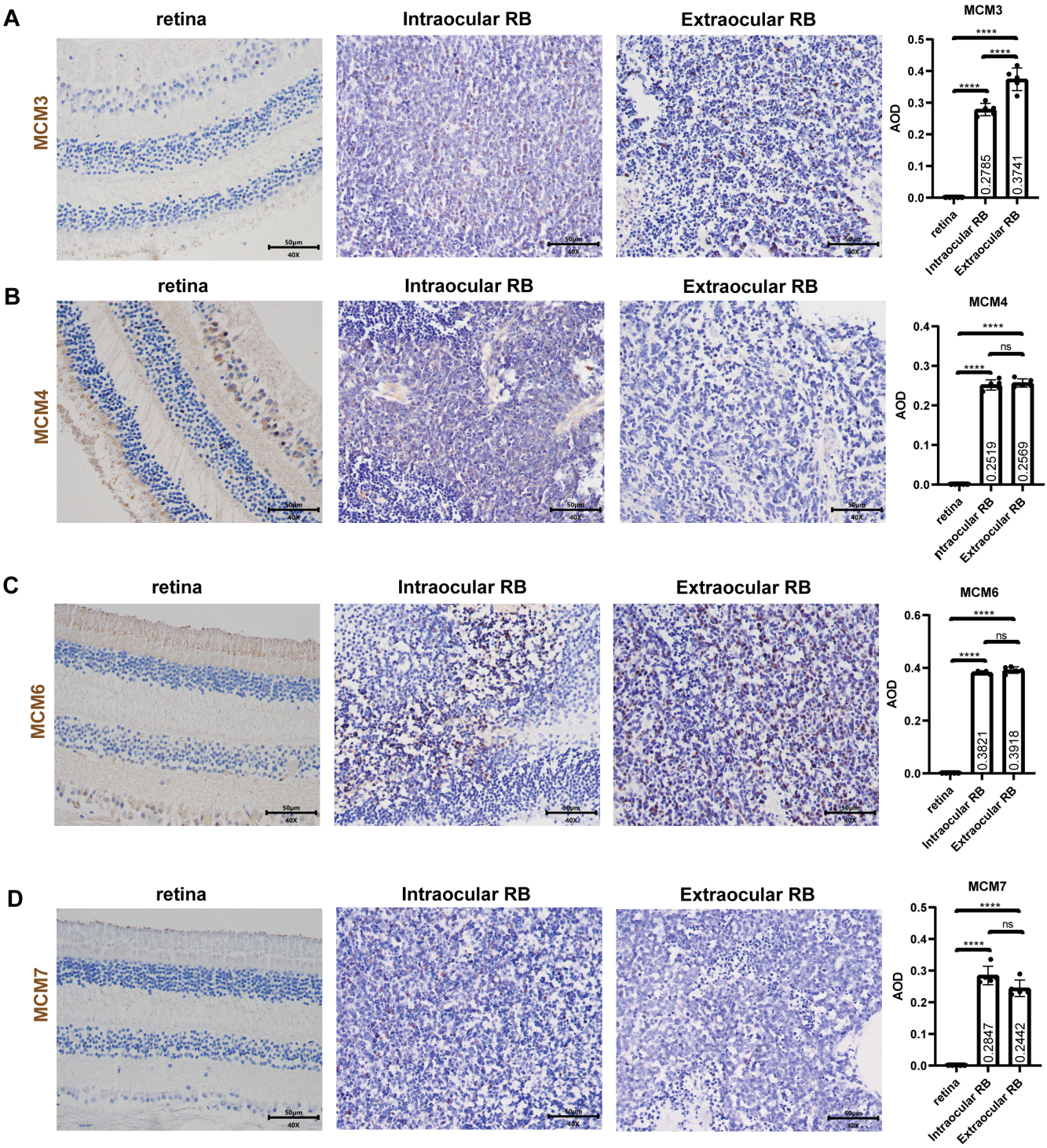

Figure 5. Immunohistochemical analysis of MCM3, MCM4, MCM6, and MCM7 in RB tissues. Immunohistochemical analysis revealing increased AOD of (**A**) MCM3, (**B**) MCM4, (**C**) MCM6, and (**D**) MCM7 in intraocular and extraocular RB samples compared with normal retina. Statistical significance denoted by $^{*}P < 0.05$, $^{**}P < 0.01$, $^{***}P < 0.001$, $^{****}P < 0.0001$ using ordinary one-way ANOVA. Ns, no significant difference.

larly because essential factors for initiating eukaryotic cell DNA replication are relatively well-established.[31] Numerous studies have demonstrated that concurrent positive expression of Ki-67, PCNA, and MCM provides a more precise reflection of cellular proliferation status, offering valuable insights into the prognosis and survival of cancer patients, and aiding in predicting the risk of tumor recurrence.[32,33] In this study, MCM6 exhibited a notable upregulation in RB across all validation assays. MCM6, a crucial DNA replication regulator, not only maintains cell cycle dynamics, but also potentially facilitates epithelial–mesenchymal transition and activates the MEK/ERK signaling pathway, contributing to

Investigative Ophthalmology & Visual Science

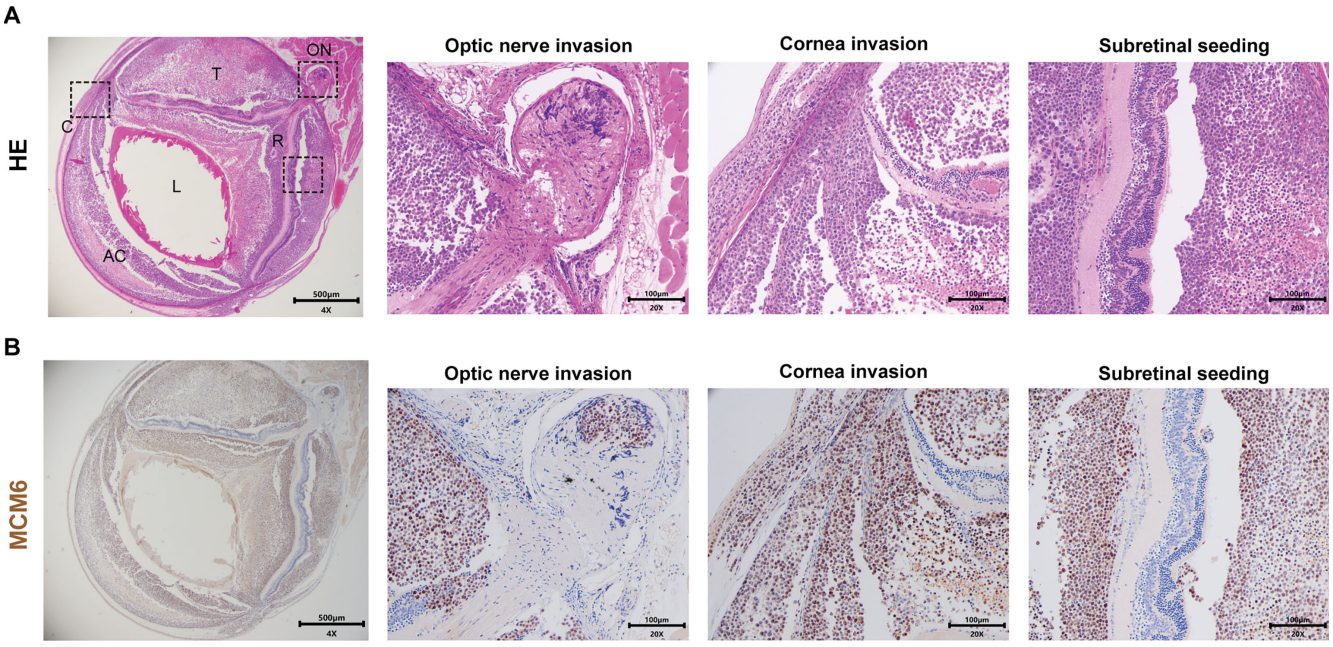

Figure 6. Validation of MCM6 expression in a murine RB model. (**A**) Histopathological and (**B**) immunohistochemical analyses in a murine model injected with WERI-Rb1 cells, illustrating tumor infiltration and significant expression of MCM6 in tumor tissue compared with noncancerous tissues. AC, anterior chamber; C, cornea; L, lens; ON, optic nerve; R, retina; T, tumor.

carcinogenesis.[9,34] Recent research has revealed substantial methylation of MCM6 in RB, indicating a potential novel mechanism for its abnormal overexpression in RB.[35]

In the progression of RB, distinct cell types, such as cone precursor-like cells, MKI67$^+$ photoreceptorness-decreased cells, and retinoma-like cells, play diverse roles and warrant attention. Cone precursor-like cells are early stage cells that have the potential to differentiate into cones and malignant cells.[21] MKI67$^+$ photoreceptorness-decreased cells represent a highly proliferative population of malignant cells.[17] Retinoma-like cells could be an intermediate cell stage between premalignant cone precursors and tumor cells.[36] The heterogeneity in MCM complex member expression across various cell types within RB sheds light on their diverse functional roles within the tumor microenvironment. Particularly, heightened expression of MCM3 and MCM7 in cone precursor-like cells and MKI67$^+$ photoreceptorness-decreased cells implied their potential involvement in regulating critical cell types pivotal to tumor progression. Furthermore, in the present study, the heightened expression of MCM3 was corroborated through IHC staining in extraocular RB samples. MCM3 has previously been reported to be significantly overexpressed in various tumors, and its specific high expression in cancer cells holds promise as a biomarker for cancer detection.[37] MCM7 plays a vital role in maintaining the initial stability of DNA replication and is involved in the ubiquitin-dependent degradation of MCM2-7 during termination.[38] Although the precise mechanisms of MCM3 and MCM7 in RB remain unclear, previous study identified interactions between the cell cycle protein cyclin D1/CDK4 kinase and components of the MCM complex, particularly emphasizing MCM3 and MCM7 as cyclin D1-binding proteins.[39]

In light of the heightened expression observed among specific members within the MCM complex in RB, it is necessary to recognize their potential significance in both diagnostic modalities and therapeutic interventions for RB. Presently, biofluids such as plasma or aqueous humor are subject to investigation for the identification of circulating tumor DNA or cell-free DNA,[40,41] respectively. This result not only simplifies the process of making informed decisions about treatment and monitoring treatment responses, but also plays a vital role in offering prognostic guidance for RB.[42–44] Notably, research has revealed an elevation of *MCM2* in cell-free RNA extracted from blood plasma in pediatric neuroblastoma,[45] especially in cases with metastasis, suggesting the potential use of minimally invasive *MCM* detection for RB diagnosis. Because MCMs exhibit upregulation in various cancers, investigations into the targeted suppression of MCMs as a strategy to impede tumor growth have been undertaken.[46,47] These studies underscore the potential therapeutic significance of MCM targeting in RB.

Our study has certain limitations. Although we observed upregulation of MCM proteins in RB, we did not explore correlations with clinical outcomes, treatment response, or patient survival. Moreover, it is important to note that the general applicability of our results may be confined to the particular patient samples included in this study, emphasizing the need for broader validation in larger and more varied populations.

In summary, this study illuminates the critical role of MCM complex members in RB. Through a comprehensive analysis using scRNA-seq data and subsequent experimental validations, we consistently observed an upregulation of MCM3, MCM4, MCM6, and MCM7 in RB, suggesting their significant functional relevance and potential implications in RB progression. Notably, MCM6 exhibited a particularly prominent elevation across various experimental validations, hinting at its promising usefulness as a valuable marker for RB. Moreover, the observed heterogeneity in MCM expression across different RB cell types underscores their

diverse functional roles within the tumor microenvironment, offering a basis for future investigations aimed at targeted therapeutic strategies.

Acknowledgments

Supported by the National Natural Science Foundation of China (82203175), and the Ocular Tumor Platform of Zhongshan Ophthalmic Center (303010406).

Disclosure: **J. Tang,** None; **Y. Liu,** None; **Z. Zhang,** None; **Y. Ren,** None; **Y. Ma,** None; **Y. Wang,** None; **J. Li,** None; **Y. Gao,** None; **C. Li,** None; **C. Cheng,** None; **S. Su,** None; **S. Chen,** None; **P. Zhang,** None; **R. Lu,** None

References

1. Dimaras H, Corson TW. Retinoblastoma, the visible CNS tumor: a review. *J Neurosci Res*. 2019;97:29–44.
2. Fabian ID, Onadim Z, Karaa E, et al. The management of retinoblastoma. *Oncogene*. 2018;37:1551–1560.
3. Munier FL, Beck-Popovic M, Chantada GL, et al. Conservative management of retinoblastoma: challenging orthodoxy without compromising the state of metastatic grace. "Alive, with good vision and no comorbidity". *Prog Retin Eye Res*. 2019;73:100764.
4. Antoneli CB, Steinhorst F, de Cássia Braga Ribeiro K, et al. Extraocular retinoblastoma: a 13-year experience. *Cancer*. 2003;98:1292–1298.
5. Moreno F, Sinaki B, Fandiño A, Dussel V, Orellana L, Chantada G. A population-based study of retinoblastoma incidence and survival in Argentine children. *Pediatr Blood Cancer*. 2014;61:1610–1615.
6. Choucair ML, Brisse HJ, Fréneaux P, et al. Management of advanced uni- or bilateral retinoblastoma with macroscopic optic nerve invasion. *Pediatr Blood Cancer*. 2020;67: e27998.
7. Zientek-Targosz H, Kunnev D, Hawthorn L, et al. Transformation of MCF-10A cells by random mutagenesis with frameshift mutagen ICR191: a model for identifying candidate breast-tumor suppressors. *Mol Cancer*. 2008;7:51.
8. Baptista D, Ferreira PG, Rocha M. A systematic evaluation of deep learning methods for the prediction of drug synergy in cancer. *PLoS Comput Biol*. 2023;19:e1010200.
9. Zeng T, Guan Y, Li YK, et al. The DNA replication regulator MCM6: an emerging cancer biomarker and target. *Clin Chim Acta*. 2021;517:92–98.
10. Noseda M, Karsan A. Notch and minichromosome maintenance (MCM) proteins: integration of two ancestral pathways in cell cycle control. *Cell Cycle*. 2006;5:2704–2709.
11. Razavi SM, Jafari M, Heidarpoor M, Khalesi S. Minichromosome maintenance-2 (MCM2) expression differentiates oral squamous cell carcinoma from pre-cancerous lesions. *Malays J Pathol*. 2015;37:253–258.
12. Li Y, Zou J, Zhang Q, et al. Systemic analysis of the DNA replication regulator MCM complex in ovarian cancer and its prognostic value. *Front Oncol*. 2021;11:681261.
13. Cai HQ, Cheng ZJ, Zhang HP, et al. Overexpression of MCM6 predicts poor survival in patients with glioma. *Hum Pathol*. 2018;78:182–187.
14. Chen R, Hu B, Jiang M, Deng W, Zheng P, Fu B. Bioinformatic analysis of the expression and clinical significance of the DNA replication regulator MCM complex in bladder cancer. *Int J Gen Med*. 2022;15:5465–5485.
15. Sun G, Li Z, Rong D, et al. Single-cell RNA sequencing in cancer: applications, advances, and emerging challenges. *Mol Ther Oncolytics*. 2021;21:183–206.
16. Liu Y, Hu W, Xie Y, et al. Single-cell transcriptomics enable the characterization of local extension in retinoblastoma. *Commun Biol*. 2024;7:11.
17. Wu C, Yang J, Xiao W, et al. Single-cell characterization of malignant phenotypes and microenvironment alteration in retinoblastoma. *Cell Death Dis*. 2022;13:438–438.
18. Lukowski SW, Lo CY, Sharov AA, et al. A single-cell transcriptome atlas of the adult human retina. *Embo J*. 2019;38:e100811.
19. Zheng GX, Terry JM, Belgrader P, et al. Massively parallel digital transcriptional profiling of single cells. *Nat Commun*. 2017;8:14049.
20. Hao Y, Hao S, Andersen-Nissen E, et al. Integrated analysis of multimodal single-cell data. *Cell*. 2021;184:3573–3587.e3529.
21. Liu H, Zhang Y, Zhang YY, et al. Human embryonic stem cell-derived organoid retinoblastoma reveals a cancerous origin. *Proc Natl Acad Sci USA*. 2020;117:33628–33638.
22. Cowan CS, Renner M, De Gennaro M, et al. Cell types of the human retina and its organoids at single-cell resolution. *Cell*. 2020;182:1623–1640.e1634.
23. Collin J, Queen R, Zerti D, et al. Dissecting the transcriptional and chromatin accessibility heterogeneity of proliferating cone precursors in human retinoblastoma tumors by single cell sequencing—opening pathways to new therapeutic strategies? *Invest Ophthalmol Vis Sci*. 2021;62:18.
24. Trapnell C, Cacchiarelli D, Grimsby J, et al. The dynamics and regulators of cell fate decisions are revealed by pseudotemporal ordering of single cells. *Nat Biotechnol*. 2014;32:381–386.
25. Ma H, Nie C, Chen Y, et al. Therapeutic targeting PLK1 by ON-01910.Na is effective in local treatment of retinoblastoma. *Oncol Res*. 2021;28:745–761.
26. Mao Y, Sun Y, Wu Z, et al. Targeting of histone methyltransferase DOT1L plays a dual role in chemosensitization of retinoblastoma cells and enhances the efficacy of chemotherapy. *Cell Death Dis*. 2021;12:1141.
27. Aubry A, Pearson JD, Huang K, et al. Functional genomics identifies new synergistic therapies for retinoblastoma. *Oncogene*. 2020;39:5338–5357.
28. Pan MR, Li K, Lin SY, Hung WC. Connecting the dots: from DNA damage and repair to aging. *Int J Mol Sci*. 2016;17:685.
29. Yang J, Li Y, Han Y, et al. Single-cell transcriptome profiling reveals intratumoural heterogeneity and malignant progression in retinoblastoma. *Cell Death Dis*. 2021;12: 1100.
30. Hashiguchi K, Matsumoto Y, Yasui A. Recruitment of DNA repair synthesis machinery to sites of DNA damage/repair in living human cells. *Nucleic Acids Res*. 2007;35:2913–2923.
31. Ishimi Y. Regulation of MCM2-7 function. *Genes Genet Syst*. 2018;93:125–133.
32. Juríková M, Danihel Ľ, Polák Š, Varga I. Ki67, PCNA, and MCM proteins: markers of proliferation in the diagnosis of breast cancer. *Acta Histochem*. 2016;118:544–552.
33. Guzińska-Ustymowicz K, Pryczynicz A, Kemona A, Czyzewska J. Correlation between proliferation markers: PCNA, Ki-67, MCM-2 and antiapoptotic protein Bcl-2 in colorectal cancer. *Anticancer Res*. 2009;29:3049–3052.
34. Liu M, Hu Q, Tu M, et al. MCM6 promotes metastasis of hepatocellular carcinoma via MEK/ERK pathway and serves as a novel serum biomarker for early recurrence. *J Exp Clin Cancer Res*. 2018;37:10.
35. Zeng Y, He T, Liu J, et al. Bioinformatics analysis of multi-omics data identifying molecular biomarker candidates and epigenetically regulatory targets associated with retinoblastoma. *Medicine (Baltimore)*. 2020;99:e23314.
36. Dimaras H, Khetan V, Halliday W, et al. Loss of RB1 induces non-proliferative retinoma: increasing genomic instability

Investigative Ophthalmology & Visual Science

correlates with progression to retinoblastoma. *Hum Mol Genet*. 2008;17:1363–1372.
37. Ha SA, Shin SM, Namkoong H, et al. Cancer-associated expression of minichromosome maintenance 3 gene in several human cancers and its involvement in tumorigenesis. *Clin Cancer Res*. 2004;10:8386–8395.
38. Moreno SP, Bailey R, Campion N, Herron S, Gambus A. Polyubiquitylation drives replisome disassembly at the termination of DNA replication. *Science*. 2014;346:477–481.
39. Gladden AB, Diehl JA. The cyclin D1-dependent kinase associates with the pre-replication complex and modulates RB.MCM7 binding. *J Biol Chem*. 2003;278:9754–9760.
40. Li HT, Xu L, Weisenberger DJ, et al. Characterizing DNA methylation signatures of retinoblastoma using aqueous humor liquid biopsy. *Nat Commun*. 2022;13:5523.
41. Jiménez I, Frouin É, Chicard M, et al. Molecular diagnosis of retinoblastoma by circulating tumor DNA analysis. *Eur J Cancer*. 2021;154:277–287.
42. Schmidt MJ, Prabakar RK, Pike S, et al. Simultaneous copy number alteration and single-nucleotide variation analysis in matched aqueous humor and tumor samples in children with retinoblastoma. *Int J Mol Sci*. 2023;24(10):8606.
43. Berry JL, Xu L, Kooi I, et al. Genomic cfDNA analysis of aqueous humor in retinoblastoma predicts eye salvage: the surrogate tumor biopsy for retinoblastoma. *Mol Cancer Res*. 2018;16:1701–1712.
44. Luo Y, Xu M, Yang L, et al. Correlating somatic copy number alteration in aqueous humour cfDNA with chemotherapy history, eye salvage and pathological features in retinoblastoma. *Br J Ophthalmol*. 2023 Mar 17:bjo-2022-322866, doi:10.1136/bjo-2022-322866. Online ahead of print.
45. Lak NSM, Seijger A, van Zogchel LMJ, et al. Cell-free RNA from plasma in patients with neuroblastoma: exploring the technical and clinical potential. *Cancers (Basel)*. 2023;15:2108.
46. Erkan EP, Ströbel T, Lewandrowski G, et al. Depletion of minichromosome maintenance protein 7 inhibits glioblastoma multiforme tumor growth in vivo. *Oncogene*. 2014;33:4778–4785.
47. Lau KM, Chan QK, Pang JC, et al. Minichromosome maintenance proteins 2, 3 and 7 in medulloblastoma: overexpression and involvement in regulation of cell migration and invasion. *Oncogene*. 2010;29:5475–5489.

Investigative Ophthalmology & Visual Science